

Zárójelentés

Újszülött csecsemők hangfeldolgozási képességei (K 101060)

A projekt során a kommunikációt megalapozó hallási feldolgozási folyamatokat vizsgáltunk egészséges, időre született újszülötteken, eseményfüggő agyi potenciálok (EAP) segítségével. Az eredményeket az egyes kérdések bontásában írjuk le.

I) Befolyásolja-e a hangkörnyezet az újszülött hallási EAP-k morfológiáját?

Megállapítottuk, hogy a hasonló eseményfüggő agy potenciál (EAP) morfológia mögött eltérő folyamatok húzódnak meg két széles spektrumú hang (fehér zaj és környezeti hangok) feldolgozásánál. Amíg a fehér zajra adott EAP válasz nem függött attól, hogy a hangot önmagában vagy egy összetett szinuszos hangokból álló hangsor részeként mutattuk-e be, a környezeti hangokra adott EAP választ szignifikánsan változtatta a hangsorbeli környezet.

Az eredményekről készült beszámolónk megjelent:

Háden, G.P., Németh, R., Török, M., Drávucz, S., & Winkler, I. (2013). Context effects on processing widely deviant sounds in newborn infants. *Frontiers in Psychology*, 4:674.

II) Magyarázható-e az újszülöttek EAP válasza deviáns ingerekre refraktórikussággal?

Megállapítottuk, hogy az újszülötteknél mérhető eltérési válasz nem magyarázható pusztán neuronális refraktórikussággal. A ritka deviáns ingereket egy olyan kontroll válasszal hasonlítottuk össze, amelyet a deviáns ingerrel azonos valószínűségi és azonos akusztikus paraméterekkel rendelkező hangok váltottak ki, melyek azonban a saját hangsorukban nem sértettek meg semmilyen szabályosságot. Az így kapott különbségi válasz ezért az emlékezeti összemérés EAP hatásának egy viszonylag tiszta becslése. Ez a kísérlet helyettesíti az eredeti terv II. kísérletét, melyet közben más kutatók már elvégeztek.

Az eredményekről készült beszámolónk megjelent:

Háden, G.P., Németh, R., Török, M., & Winkler, I. (2016). Mismatch response (MMR) in neonates: beyond refractoriness. *Biological Psychology*, 117, 26–31.

III) Az újszülött csecsemők felbontják-e a hangokat egymástól független ingertulajdonságokra?

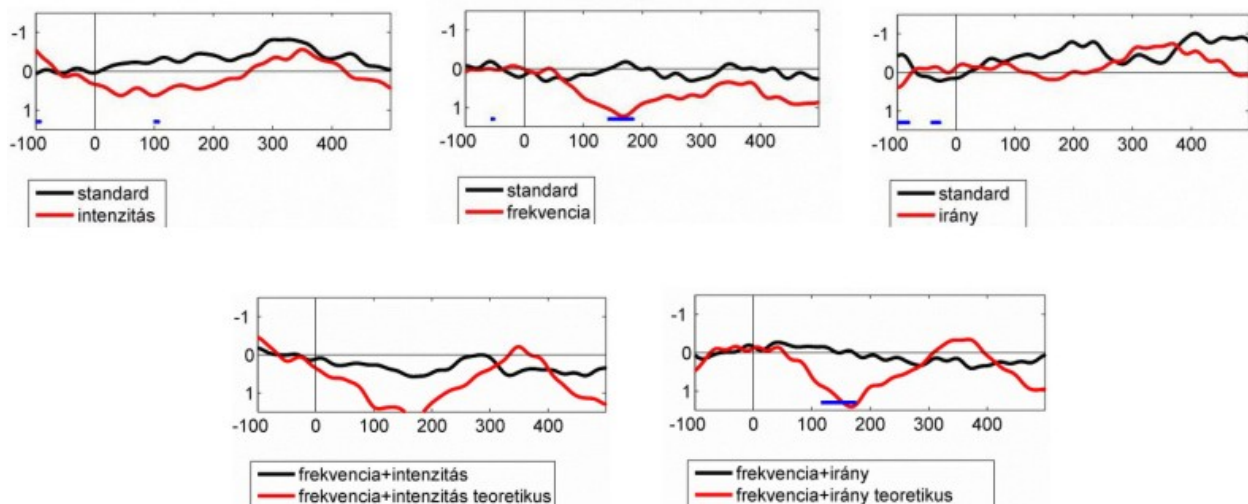
Ennek a kérdésnek a megválaszolásához először bizonyítani kellett, hogy az újszülöttek érzékenyek egy korábban nem vizsgált hang-tulajdonságra, a hangforrás helyére. Megállapítottuk, hogy az újszülött csecsemők feldolgozzák a horizontális irányú hangforrás lokalizáció két legfontosabb jelzőmozzanatát, a fülek közötti idő és hangerősség különbséget. Azonban, a jelzőmozzanatok szenzoros felbontása jelentősen alacsonyabb a felnőttekhez képest. Újszülöttek a hangforrások irányának eltérést csak redundáns jelzőmozzanatok (egyik vs. másik fül, vagy valódi térben elhelyezett hangforrások) esetén detektálják megbízhatóan.

Az eredményekről készült beszámolónk megjelent:

Németh, R., Háden, G.P., Török, M., & Winkler, I. (2015). Processing of horizontal sound localization cues in newborn infants. *Ear and Hearing*, 36(5), 550-556.

A következő lépésben a hangmagasság és a) a hangerősség illetve b) a hangforrás helye tulajdonságok független reprezentációját vizsgáltuk meg oly módon, hogy összehasonlítottuk a ritka, mindkét tulajdonságban a gyakori ingertől eltérő hangokra adott választ a két külön-külön megjelenő eltérésre adott válaszok összegével. Az összeadott (elméleti) és a valós válaszok egyenlősége a két tulajdonság függetlenségére utal. Felnőtt adatok alapján, a hangmagasság és a hangerő között összefüggést, a hangmagasság és a hangforrás helye között függetlenséget vártunk.

Az eredmények mindkét esetben jelentős eltérést mutattak az elméleti és a valós válaszok között (1. ábra). Ez arra utal, hogy az újszülöttek nem bontják fel a hangokat független hangtulajdonságok mentén. Az eredmények értékelése még folyamatban van. A későbbiekben ezekről cikkben kívánunk beszámolni.



1. ábra. Felső sor: A gyakori hangingerektől különböző tulajdonságokban (intenzitás: bal oldal; hangmagasság: közép; hangforrás helye: jobb oldal) eltérő ritka hangokra adott átlagolt EAP válaszok újszülött csecsemőknél (n=22). A gyakori ingert fekete, a ritka ingert piros vonallal ábrázoltuk. **Alsó sor:** Az egy tulajdonságban eltérő ritka hangingerekre adott válaszok összegének és az egyszerre két tulajdonságban eltérő ritka hangokra adott EAP válaszok összehasonlítása. Az ingerre adott választ fekete, a két egy-egy tulajdonságban eltérő ingerre adott válasz összegét piros vonallal ábrázoltuk.

IV) Érzékenyek-e az újszülött csecsemők a párhuzamosan működő hangforrások szétválasztásának azonnali jelzőmozzanataira?

Megállapítottuk, hogy újszülött csecsemők érzékenyek a hallási láncrea bontás két azonnali jelzőmozzanataira, az elhangolt harmonikusra és az eltérő hangkezdetre. Amennyiben összetett szinuszos hangok valamelyik harmonikusát elhangoljuk, vagy a többihez képest késleltetjük, akkor az EAP-ben megjelenik egy olyan eltérés, amely analógiába hozható, a felnőtteknél talált tárgyhoz kötött negativitás (TKN) komponenssel.

Az eredményekről készült beszámolónk megjelent:

Bendixen, A., Háden, G.P., Németh, R., Farkas, D., Török, M., & Winkler, I. (2015). Newborn infants detect cues of concurrent sound segregation. *Developmental Neuroscience*, 37(2), 172-181.

V) Reprezentálják-e az újszülöttek a hangmagasság változások trendjét?

Megállapítottuk, hogy újszülött csecsemők detektálják hangmagasság trendek megtörését. Monoton csökkenő hangmagasságú hangokból álló hangsorba ritkán beiktatott hangismétlések kiváltják a várható hangtól való eltérést jelző eltérési negativitással (EN) analóg EAP komponenset. Az eredmények azt is megmutatták, hogy az újszülöttek a változás detektált iránya alapján előrejelzéseket tesznek a következő hang várható magasságára.

Az eredményekről készült beszámolóink megjelent:

Háden, G.P., Németh, R., Török, M., & Winkler, I. (2015). Predictive processing of pitch trends in newborn infants. *Brain Research*, 1626, 14-20.

VI) Detektálják-e az újszülöttek a hangsorok kezdetét, végét és a hangsor ütemének változását?

Megállapítottuk, hogy újszülött csecsemők detektálják rövid hangsorok kezdetét, első ütemváltozását és befejezését. Az eredmény azt mutatja, hogy már újszülöttek is rendelkeznek a "turn-taking" és a beszéd-ütem adaptációhoz szükséges hallási perceptuális képességekkel.

Az eredményekről készült beszámolóink megjelentek:

Háden, G.P., Honing, H., Török, M., & Winkler, I. (2015). Detecting the temporal structure of sound sequences in newborn infants. *International Journal of Psychophysiology*, 96(1), 23-28.

Háden, G.P., Honing, H., & Winkler, I. (2012). Newborn infants are sensitive to sound timing. In E. Cambouropoulos, C. Tsourgas, P. Mavromatis and K. Pastiadis (Eds.), *Proceedings of the 12th International Conference on Music Perception and Cognition and the 8th Triennial Conference of the European Society for Cognitive Sciences of Music* (pp. 378-379), July 23-28, 2012, Thessaloniki, Greece.

A hangok időzítésére való érzékenység fejlődésének vizsgálata során megállapítottuk, hogy két és négy hónapos csecsemők reprezentálják a hangsorok bemutatási ütemét: az ingerek közötti idő ritkán történő lerövidítése kiváltja az automatikus előrejelzések megsértésének megfelelő EAP-eket. Az EAP-k morfológiájában két és négy hónapos kor között található különbségek jelzik a feldolgozási folyamatok fejlődését.

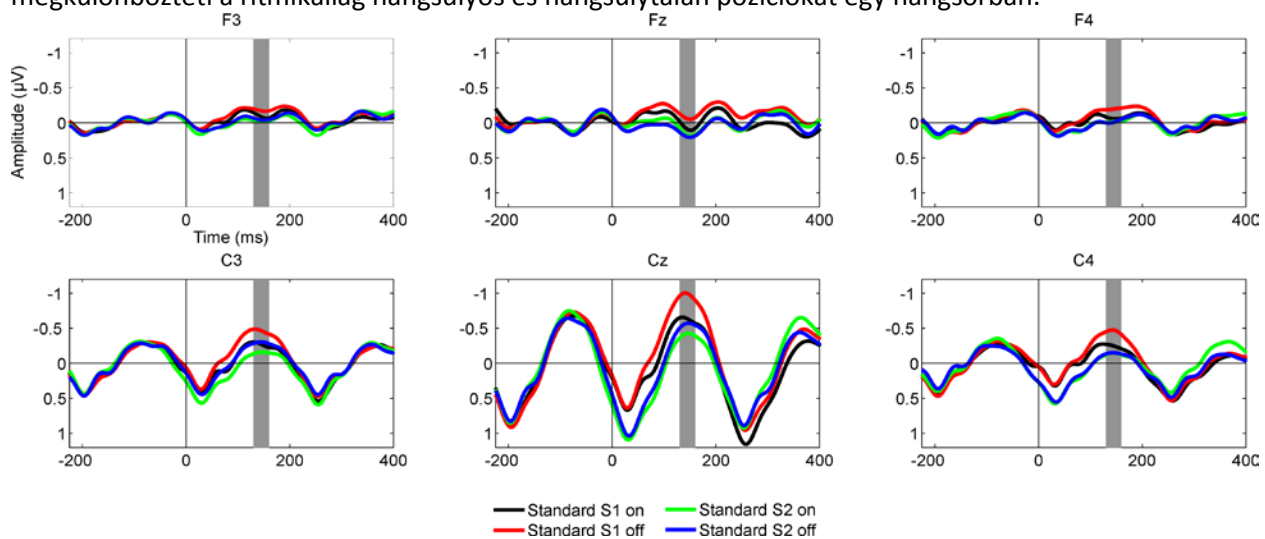
Az eredményekről készült beszámolóink megjelent:

Otte, R.A., Winkler, I., Braeken, M.A.K.A., Stekelenburg, J.J., van der Stelt, O., & Van den Bergh, B.R.H. (2013). Detecting violations of temporal regularities in waking and sleeping two-month-old infants. *Biological Psychology*, 92(2), 315-322.

van den Heuvel, M.I., Otte, R.A., Braeken, M.A.K.A., Winkler, I., Kushnerenko, E., & Van den Bergh, B.R.H. (2015). Differences between human auditory event-related potentials (AERP) measured at 2 and 4 months after birth. *International Journal of Psychophysiology*, 97(1), 75–83.

VII) Ritmikailag hangsúlyos és hangsúlytalan hangok feldolgozása újszülött csecsemőknél

Kidolgoztunk egy olyan ingerparadigmát, amellyel egy ingersorban a ritmikailag hangsúlyos és hangsúlytalan pozíciókban kiváltott agyi válaszok hasonlíthatóak össze, akusztikailag jól kontrollált környezetben. Az elrendezésben zongora és csembaló hangok felváltva követik egymást és a sorozat kezdő hangja határozza meg, hogy a kettő közül melyik hangot észleljük hangsúlyosnak. Eredményeink (lásd 2. ábra) alapján az újszülött hallórendszer e minimális kontextuális információ alapján is megkülönbözteti a ritmikailag hangsúlyos és hangsúlytalan pozíciókat egy hangsorban.



2. ábra. Átlagolt (n=24) EAP-k újszülött csecsemőknél hangsúlyos (on) és hangsúlytalan (off) pozícióban megjelenő zongora (S1) és csembaló (S2) hangokra. A szürke sáv az EAP amplitúdó mérési ablakát jelzi.

Az eredményekről beszámoló cikk megírását megkezdtük. Egy előadást már tartottunk az eredményekről:

Háden, G.P., Simon, J., Winkler, I.: Rhythmic context affects deviant processing in newborn infants. BACN, The British Association for Cognitive Neuroscience (BACN) annual meeting, September 12-14, 2016, Budapest Hungary.

VIII) Születési és anyai változók hatása csecsemők agyi aktivitására

A fogantatástól a megszületésig eltelt idő befolyásolja az újszülöttek EEG-ből számított nyugalmi funkcionális hálózatának struktúráját. Az elemzéshez elsőként alkalmaztuk újszülötteknél a minimális feszítő fák módszerét. A módszer lehetővé tette számunkra a hálózatok globális tulajdonságainak vizsgálatát. A frontális és parietális hálózatok topológiai tulajdonságai összefüggést mutattak a terhesség hosszával. Ez alapján arra következtethetünk, hogy az agyi funkcionális hálózatok változása összefügg az agy érésével: a centralizált hálózatok decentralizáltabb hálózatoknak adják át a helyüket.

Az eredményekről készült cikk jelenleg revízió alatt áll (lásd a csatolt kéziratot):

Tóth, B., Hádén, G.P., Urbán, G., Molnár M., Török, M., Stam, C.J., & Winkler, I. (under revision). Resting-state EEG functional connectivity in newborn infants. *Human Brain Mapping*.

Az anyai gondosság és szorongás hatással vannak a bejósolhatatlan hang-változások által kiváltott EAP válaszokra 9 hónapos csecsemőknél. Megállapítottuk, hogy az anyai gondosság csökkenti, a szorongás növeli az ilyen válaszokat. Ezt úgy értelmeztük, hogy az anyai gondoskodás hatással van arra, hogy a váratlan események milyen mértékű figyelmi elterelődést váltanak ki a csecsemőben.

Az eredményekről készült beszámolóink megjelent:

van den Heuvel, M.I., Donkers, F.C.L., Winkler, I., Otte, R.A., & Van den Bergh, B.R.H. (2015). Maternal mindfulness and anxiety during pregnancy affect infants' neural responses to sounds. *Social Cognitive and Affective Neuroscience*, 10(3), 453-460.

IX) Elméleti összefoglalók

Összefoglaló elemzést közöltünk arról, hogyan válik szét az akusztikus eltérés és az újdonság feldolgozása az élet első évében.

Kushnerenko, E.V., Van den Bergh, B.R.H., & Winkler, I. (2013). Separating acoustic deviance from novelty during the first year of life: A review of event-related potential evidence. *Frontiers in Psychology*, 4:595.

Elemeztük az újszülött csecsemők hallási képességeinek mintázatát. Arra a következtetésre jutottunk, hogy e képességek jelentős része a hangokkal történő kommunikáció, azon belül is a dialógusok felépítésének és fenntartásának szolgálatában áll.

Winkler, I. (2015). Előbb az összetett, később az egyszerű: Csecsemők magasabb szintű hangfeldolgozási képességei a beszédértés előtti időszakban. *Magyar Pszichológiai Szemle*, 70(4), 675-721.

Összefoglalás

A pályázat megvalósítása során haladást értünk el az újszülött csecsemők hallási képességeinek feltérképezésében. Ezekre, és korábbi vizsgálatokra támaszkodva előre léptünk e képességek funkcionális értelmezésében is.

Egy eltéréssel, amelyet a szakirodalom menet közbeni fejlődése indokolt, megvalósítottuk a tervezett kísérleteket. Az eredmények többségét a pályázati időszakban publikáltuk; a fennmaradó vizsgálatok eredményeinek publikációja pedig folyamatban van. Néhány területen, nemzetközi együttműködés segítségével túlteljesítettük a pályázatban vállalt feladatokat.

Melléklet:

Tóth, B., Hádén, G.P., Urbán, G., Molnár M., Török, M., Stam, C.J., & Winkler, I. (under revision). Resting-state EEG functional connectivity in newborn infants. Kézirat.



Large-scale network organization of EEG functional connectivity in newborn infants

Journal:	<i>Human Brain Mapping</i>
Manuscript ID	Draft
Wiley - Manuscript type:	Research Article
Date Submitted by the Author:	n/a
Complete List of Authors:	Tóth, Brigitta; Research Centre for Natural Sciences, Hungarian Academy of Sciences, Institute of Cognitive Neuroscience and Psychology, Urbán, Gábor; Institute of Cognitive Neuroscience and Psychology, Research Centre for Natural Sciences, Hungarian Academy of Sciences, Budapest, Hungary, Háden, Gabor; Institute of Cognitive Neuroscience and Psychology Research Center for Natural Sciences HAS Márk, Molnár; Research Centre for Natural Sciences, Hungarian Academy of Sciences, Institute of Cognitive Neuroscience and Psychology, Török, Miklós; Military Hospital, Department of Obstetrics-Gynaecology and Perinatal Intensive Care Unit Stam, Cornelis; VU University Medical Center, Clinical Neurophysiology; Wnkler, István; Research Centre for Natural Sciences, Hungarian Academy of Sciences, Institute of Cognitive Neuroscience and Psychology,
Keywords:	Electroencephalography, neonate, functional connectivity, network analysis, graph theory, Minimum Spanning Tree

SCHOLARONE™
Manuscripts

1
2
3 **Full title:** Large-scale network organization of EEG functional connectivity in newborn infants
4

5 **Brigitta Tóth^{1*}, Gábor Urbán^{1,2}, Gábor P. Hádén¹, Márk Molnár¹, Miklós Török⁴, Cornelis Jan Stam⁵, and**
6
7 **István Winkler¹**
8

9
10 ¹Institute of Cognitive Neuroscience and Psychology, Research Centre for Natural Sciences, Hungarian
11 Academy of Sciences, Budapest, Hungary
12

13 ²Department of Cognitive Science, Faculty of Natural Sciences, Budapest University of Technology and
14 Economics, Budapest, Hungary
15

16 ⁴Department of Obstetrics-Gynaecology and Perinatal Intensive Care Unit, Military Hospital, Budapest, Hungary
17

18 ⁵Department of Clinical Neurophysiology, VU University Medical Center, Amsterdam, Netherlands
19

20 ***Correspondence to:**

21 Brigitta Tóth
22 Institute of Cognitive Neuroscience and Psychology
23 Hungarian Academy of Sciences
24 Magyar tudósok körútja 2.
25 Budapest 1117
26 Hungary
27 E-mail: toth.brigitta@ttk.mta.hu
28
29
30

31 **Short title:** Functional connectivity in the newborn brain
32

33 **Keywords:** Electroencephalography, neonate, functional connectivity, network analysis, graph theory, Minimum
34 Spanning Tree
35
36
37
38
39
40
41
42
43
44
45
46
47
48
49
50
51
52
53
54
55
56
57
58
59
60

Abstract

The organization of functional brain networks changes across human lifespan. The present study analyzed functional brain networks in healthy full-term infants (N = 139) within 1-6 days from birth by measuring neural synchrony in EEG recordings during quiet sleep. Large-scale phase synchronization was measured in six frequency bands with the Phase Lag Index. Macroscopic network organization characteristics were quantified by constructing unweighted minimum spanning tree graphs. The cortical networks in early infancy were found to be significantly more hierarchical and had a more cost-efficient organization compared to MST of random control networks, more so in the theta and alpha than in other frequency bands. Frontal and parietal sites acted as the main hubs of these networks, the topological characteristics of which were associated with gestation age (GA). This suggests that individual differences in network topology are related to cortical maturation during the prenatal period, when functional networks shift from strictly centralized toward segregated configurations.

1. Introduction

Efficient communication between brain regions in both micro- and macroscopic scales is essential for healthy cognitive functioning [Bassett et al., 2009; van den Heuvel et al., 2009; Varela et al., 2001; Uhlhaas and Singer, 2010]. The establishment of synaptic connections between cortical neurons forming highly organized cortical networks has been suggested as a hallmark of neuronal maturation [Boersma et al., 2011]. Previous infant studies found that genetic factors and sensory input are both crucial for the development of cortical networks [for a review, see Khazipov and Luhmann, 2006]. Neuronal communication between brain areas, the temporal coupling/dependency between spatially remote neuronal assemblies (termed “functional connectivity”; FC), has been shown to develop throughout the human lifespan [Fransson et al., 2007, Uhlhaas et al., 2009; Uhlhaas et al., 2010]. Therefore, it is important to determine its characteristics at birth, the point at which the environmental stimulation radically changes from that of the preceding fetal period. The aim of the present study was to track the organization of large-scale functional brain networks in newborn infants during quiet sleep and explore its relationship with gestational age (index of prenatal maturation) and variables characterizing possible prenatal influences on brain maturation, including some general clinical risk factors of the mother and the offspring.

EEG amplitude coherence and phase synchronization of neural rhythms are the most widely used methods for determining the strength of FC in spontaneous brain activity during rest or sleep. The large majority of studies investigating the development of FC in infancy have assessed either 1) FC differences between preterm or extremely low birth-weight infants and full-term newborns (Pereda et al., 2006, Gonzalez et al., 2011, Meijer et al., 2014, Grieve et al, 2008, Omidvarnia et al. 2014) or 2) longitudinal changes in FC following preterm birth (Jennekens et al., 2012, Myers et al., 2012). One important result of these studies is the observations of rapid increase in fronto-parietal connectivity in preterm population from day one to three (Schumacher et al., 2015) and stronger connectivity in healthy relative to extremely low birth-weight newborns (Grieve et al, 2008). Although these and similar results clearly demonstrate that FC patterns are potential indicators of cortical immaturity, yet little is known about the effects of prenatal development on FC in healthy newborn infants.

Functional brain networks can be described as graphs, an abstract mathematical description of the network's elements and their interactions [for a review, see Stam, 2014; Stam and van Straaten, 2012]. Graph theoretical modelling has been useful for investigating the organizational principles of brain networks (for a review, see Varela et al., 2001). In healthy adults, in rest or no-task condition, EEG/MEG functional networks take the form of the cost-efficient “small-world” organization, which produces optimal ratio of direct communication between closely spaced and separated brain areas [Stam and van Straaten, 2012]. The small-world network organization combines the high-level clustering of ordered regular networks (which enable fast information flow within local subnetworks) with the short path length of random networks (which enable efficient large-scale

1
2
3 integration of subnetworks). These neuronal networks also display hierarchical topology (see de Haan et al.,
4 2012; van den Heuvel and Pol, 2010) and include densely connected 'hub' regions, which can serve as
5 coordination centers [Achard et al., 2006].
6
7

8 So far, only few studies assessed the early development EEG brain networks in healthy newborns
9 (Tokariev et al., 2015, Omidvarnia et al. 2014). During the first ca. 2 weeks after birth an increase in
10 interhemispheric phase synchrony was observed together with a concurrent decrease in the ratio of intra-
11 /interhemispheric connections in the low delta range (Tokariev et al., 2015). Another study (Omidvarnia et al.
12 2014) showed that the FC network organization during late gestation exhibits salient, spatially selective
13 developmental trajectories: subnetwork clustering increases in anterior and decreases in posterior cortical areas,
14 evidenced both at lower (3–8 Hz) and even stronger at the higher frequencies (5–18 Hz). These results represent
15 network reorganization resulting from maturation or the change in external stimulation. Subnetworks further
16 develop later during infancy and they are gradually differentiated during childhood, suggesting a relationship with
17 the development of cognitive abilities [Ferreira and Busatto, 2013; van den Heuvel and Pol, 2010]. From a graph-
18 theoretical perspective, FC between 5 and 7 years of age already exhibits the economical trade-off between high
19 level clustering and short path length [Boersma et al., 2011; Fair et al., 2008; Micheloyannis et al., 2006; Power
20 et al., 2010; Supekar et al., 2009, Smit et al., 2012, Bathelt et al., 2013]. fMRI studies of structural and functional
21 connectivity in typically developing infants and children consistently observed that 1) after birth, the infant brain
22 first develops strong local connectivity; 2) later, the focus shifts gradually toward stronger long-distance
23 connectivity by strengthening the distant and weakening the local connections [Barry et al., 2004; Gong et al.,
24 2009; Thatcher, 1992; Thatcher et al., 2008, Fair et al., 2008; Lebel et al., 2008; Power et al., 2010; Supekar et
25 al., 2009; Yap et al., 2011].
26
27
28
29
30
31
32
33
34
35
36
37

38 In the present study, EEG has been recorded during quiet sleep [Prechtl, 1974] in healthy newborn
39 infants born to term. The most frequent quiet sleep state was chosen because it is easily identifiable and it is the
40 dominant vigilance state of the newborns; further, it has been associated with postmenstrual age (Duffy et al.
41 2003; Dulce et al., 2007). The characteristic features of FC have been extracted from EEG by calculating phase
42 synchronization (measured as phase lag index, PLI; [Stam et al., 2007]) and represented using the graph-
43 theoretical measures of minimum spanning tree (MST) topologies [Boersma et al., 2013, Stam and van Straaten,
44 2012]. The PLI measure reduces the effects of volume conduction (the effects of common sources on the EEG
45 signal) and it is (largely) independent of the reference electrode [Martin and Chao, 2001]. PLI has been
46 previously employed in measuring newborn infants' EEG-based FC (Gonzalez et al., 2011). Medical/biological
47 data about the gestation age, the mother, and the infant were collected and their relationship with the
48 characteristics of the functional networks was determined for assessing their possible association with brain
49 maturation. In particular, we expected that 1) the topology of neuronal FCs will differ as a function of the
50 underlying oscillatory frequencies and 2) longer gestation age, higher birth-weight, and optimal cardiovascular
51
52
53
54
55
56
57
58
59
60

measures of the mother will result in more mature FC topologies (closer to the organization that combines the optimal ratio between functionally integrated and segregated FCs) in the infants.

2. Materials and methods

2.1. Participants

EEG was recorded in 164 healthy, full-term (gestation age (GA) 36 weeks and above) newborn infants (90 male) during day 1-6 postpartum. Data of 25 infants were excluded based on the criterion of retaining overall 140 seconds of EEG signal after artifact rejection (at least 35 epochs of 4096 ms duration). Thus, 139 healthy, full-term new-born infants (76 male) were included in the final sample. Table 1 summarizes descriptive statistics of medical/biological measures, whereas Supplementary table 1 shows the distribution of categorical data in our sample.

2.2. Procedure, Electroencephalographic recording

EEG was recorded in a dedicated experimental room at the Department of Obstetrics-Gynecology and Perinatal Intensive Care Unit, Military Hospital, Budapest. Informed consent was obtained from one or both parents. The mother of the infant could opt to be present during the recording. The study was conducted in full accordance with the World Medical Association Helsinki Declaration and all applicable national laws; it was approved by the relevant ethics committee: Medical Research Council – Committee of Scientific and Research Ethics (ETT-TUKEB), Hungary. The infants in our sample participated in one or more other EEG studies on sound processing within the same session. The EEG data reported here was always recorded first within the session.

Five minutes of spontaneous EEG was recorded during quiet sleep with Ag/AgCl electrodes attached to the scalp at the Fp1, Fp2, Fz, F3, F4, F7, F8, T3, T4, Cz, C3, C4, Pz, P3, P4 locations according to the International 10-20 system. The reference electrode was placed on the tip of the nose and the ground electrode on the forehead. Eye movements were monitored with two bipolarly connected electrodes: one placed lateral to the outer canthus of left eye and the other above the left eye. EEG was digitized with 24 bit resolution at a sampling rate of 1 kHz by a direct-coupled amplifier (V-Amp, Brain Products GmbH). The signals were on-line low-pass filtered at 110 Hz. The impedance of the electrodes was kept below 20 k Ω . Infants' sleep state was determined based on behavior criteria according to Anders et al. (1971). Only infants that were in quiet sleep for the whole 5 minute duration were included in the study. In addition to the behavioral criteria employed, the EEG

1
2
3 signal was visually inspected. If movement related artefacts were present, the data was rejected from the further
4 analysis (ensuring that muscle tension was tonic, respiration regular, and eyes movements absent).
5
6

7 **2.3. EEG data analysis**

8
9 EEG signals were off-line filtered (band-pass, Hamming windowed Fast Fourier Transform) in the 0.5-45
10 Hz frequency range. EEG data was analyzed by extracting 4096 ms long epochs (minimum of 35 epochs per
11 participant; average number of epochs/participant: 55.54, SD = 14.88). The strength of FC was quantified by
12 measuring phase synchronization between EEG channels in five frequency bands (delta: 0.5-4 Hz; theta: 4-8 Hz,
13 lower alpha: 8-10 Hz, upper alpha: 10-12 Hz, beta: 13-30 Hz, gamma 30-45 Hz), separately for each epoch. The
14 level of FC between any two signals is defined as the phase lag synchronization strength measured by the phase
15 lag index (PLI). PLI reflects the consistency by which one signal is phase leading or lagging with respect to
16 another signal [a detailed mathematical description can be found in Stam et al., 2007]. PLI is expressed as a
17 value between 0 (random phase difference: minimum strength of functional connectivity) and 1 (constant phase
18 difference: maximum strength of functional connectivity). PLI was calculated by using the BrainWave software
19 version 0.9.151.5 [available at <http://home.kpn.nl/stam7883/brainwave.html>]. Graph construction was based on
20 the full connectivity matrix constructed from the PLI values obtained for each pair of electrodes.
21
22
23
24
25
26
27
28
29

30 **2.4. Graph-theoretical analysis**

31
32 In order to investigate the global topological organizational of infant functional brain networks, the graph
33 theoretical representation of the functional connectivity matrix was created by the MST approach [Boersma et al.,
34 2013, Stam and van Straaten, 2012]. The MST graph of a connectivity matrix is a graph in which all nodes
35 (electrodes) are connected using the strongest available connections and without forming loops. As a
36 consequence, only one path connects any pair of nodes. MST graphs were generated separately for each infant,
37 epoch and frequency band. Graph metrics computed from MSTs are strongly related to those computed from the
38 original network as characterized by weighted connections between each pair of nodes [Tewarie et al., 2015].
39 The characteristics extracted from the graphs derived by the MST approach have been successfully employed for
40 describing FC network properties (e.g. hierarchical structure, degree distribution etc.) of healthy adults and
41 patient groups with neurodegenerative disorders, such as epilepsy and multiple sclerosis (for review, see Stam et
42 al., 2014). For the current analysis, MST connectivity networks were derived by the Kruskal's algorithm [Kruskal,
43 1956]. Following the construction of MSTs, global and node-specific network characteristics (see Figure 1) were
44 quantified based on the measures described by Stam et al. (2014). "Degree Centrality" (DEG) is the number of
45 edges connected to a node. "Betweenness Centrality" (BC) is a measure of the node's 'hubness' within the
46 network. It is defined as the normalized fraction of all shortest paths connecting two nodes that pass through the
47 particular node [for detailed mathematical description see Newman and Girvan, 2010; Stam et al., 2014]. The
48
49
50
51
52
53
54
55
56
57
58
59
60

1
2
3 DEG and BC measures were calculated for each node separately and the maximum values within each MST
4 were included in the statistical analyses as global characteristics of the MST (MaxDEG and MaxBC,
5 respectively). “Leaf Fraction” (LF) is the number of nodes with only 1 connected edge divided by the total number
6 of nodes in the MST. “Diameter” (DIAM) is the largest distance between any two nodes within the MST, where
7 distance refers to the minimum number of edges required to proceed from one node to another (the shortest
8 path). “Tree Hierarchy” (TH) assesses how hierarchical a given network is compared to the so called ‘star-like
9 network organization’. The calculation of TH is based on the values of maximum BC and Leaf Fraction [for a
10 detailed mathematical description, see Boersma et al., 2013, and Tewarie et al., 2015]. TH ranges from 0
11 (indicating a line-like topology) to 1; for the star-like topology, TH approaches 0.5. The optimal TH is somewhere
12 between a path and a star like topology; the higher the TH, the better the tradeoff between integration and
13 differentiation in an MST. MST network characteristics values were normalized by dividing them by the number of
14 EEG channels. The global MST network characteristics were averaged across epochs, separately for each infant
15 and frequency band.

16
17
18
19
20
21
22
23
24
25 PLEASE INSERT FIGURE 1 HERE
26
27
28

29
30 For assessing whether the graph-theory based descriptions of the FCs represent common tendencies
31 for the current group of infants, brain network characteristics were compared with those of referential random
32 networks. Random-network characteristics were calculated by randomly permuting the PLI values within the
33 connectivity matrix, separately for each epoch, infant, and frequency band. Random-network MST graphs were
34 quantified the same way as was described above for the actual EEG data.

35
36
37
38 MST graphs may also carry information regarding the topography of FCs common within the group of
39 infants. Therefore, we assessed the distribution of the node characteristics Betweenness Centrality and Degree
40 Centrality over the scalp. Commonalities between the MSTs should result in non-uniform scalp distributions of
41 these node characteristics. For each node (electrode), infant, and frequency band, the average DEG and BC
42 values were computed and their scalp distributions were then calculated.

43 44 45 46 47 **2.5. Statistical analysis**

48
49 Statistical analysis was performed with the SPSS software package [version 20.0; IBM Corp., 2011]. For
50 testing whether the observed functional networks represent characteristics of the infant brain, repeated-measures
51 Analyses of Variance (ANOVA) were used to compare the characteristics of random network and the infant FC
52 networks, separately for each frequency band (NETWORK TYPE × BAND) and each MST network characteristic
53 (MaxDEG, MaxBC, LF, DIAM, and TH). Greenhouse-Geisser correction was employed to correct for sphericity
54 violations. In this case, Mauchly’s W (ϵ) and the significance value of the sphericity test (p_ϵ) are given. Effect
55
56
57
58
59
60

1
2
3 sizes (partial eta squared, η^2) are also shown. For testing the scalp distribution of node indices of the infant brain
4 networks, one-way ANOVAs were used to compare the spatial characteristics of these node measures (NODE
5 LOCATION), separately for each frequency band and network characteristic (MaxDEG, MaxBC).
6
7

8 By following a data-driven Forward algorithm¹, linear regression models [Pearson, 1895] were
9 constructed for assessing the relationship between medical/biological data and functional network characteristics
10 (DEGMax, BCMax, LF, DIAM, and TH), separately for each frequency band. To avoid distorted results we
11 controlled the skewness value of variables with the “rule of thumb” threshold of -1.0 1.0 [Pearson, 1895]. This
12 type of filtering allowed us to enter into these analyses the following variables: “gestation age” (GA), “infant’s birth
13 weight” (BW), “infant’s age at the time of the recording” (IA), “mother’s age” (MA), “mother’s postpartum weight”
14 (MW), and “mother’s height” (MH). Because linear regression models are not sensitive to multiple comparisons,
15 the emerging patterns of relationships between the medical/biological and network-describing variables do not
16 run the danger of producing false positive results due to multiple probabilistic tests [Gelman, Hill, and Yajima,
17 2012].
18
19
20
21
22
23
24
25

26 3. Results

27
28 To illustrate the general FC network topologies, a group-averaged connectivity matrix was constructed
29 for each frequency band. The visualized MSTs of these mean matrices are shown in Figure 2. Note that the
30 topology of the EEG networks varies across frequency bands (see detailed statistical results below). In the delta,
31 theta and alpha frequency bands, fronto-central nodes (Fz and Cz) showed the highest centrality values and
32 strongest functional connections. In the faster frequency bands, the nodes of the temporal lobe displayed the
33 highest centrality values and strongest functional connectivity. The infant FC networks are quite hierarchical in all
34 frequency bands (see detailed statistical analysis below): they are generally organized into 3-4 hierarchical layers
35 (see Figure 2.) with most of the nodes being functionally linked to only one of the nodes in the first layer.
36 Therefore the functional connections of infant brain networks appear to be organized in a highly centralized
37 manner.
38
39
40
41
42
43
44
45

46 PLEASE INSERT FIGURE 2 HERE

47 48 49 3.1. Comparing network characteristics between infant FC networks and corresponding random 50 networks 51

52
53
54
55
56
57 ¹ The Forward algorithm adds independent variables into the model as long as it significantly changes the value of explained
58 variance. In the current analysis, other linear regression methods (Backward, Stepwise, etc.) yielded the same results.
59 Therefore, we do not mention these alternatives.
60

1
2
3 **Maximal Degree.** The MaxDEG values were significantly higher for the infant FC networks than for the
4 random networks (main effect of NETWORK TYPE: see Table 2). The BAND×NETWORK TYPE interaction was
5 significant, because unlike for random networks, MaxDEG significantly varied across frequency bands for the
6 infant FC networks ($p < .001$ in all pairwise comparisons between the gamma and any other band as well as
7 between the delta/beta and the theta/lower-alpha/higher-alpha comparisons).
8
9

10
11 **Maximal Betweenness Centrality.** The MaxBC values were significantly higher for the infant FC
12 networks than for the random networks. The BAND×NETWORK TYPE interaction was significant, because unlike
13 for random networks, MaxBC significantly varied across frequency bands for the infant FC networks ($p < .001$ in
14 all pairwise comparisons between the gamma and any other band as well as between the delta/beta and the
15 theta/lower-alpha/higher-alpha comparisons, except for the comparison between the delta and the upper alpha
16 band, which yielded a p value of .002).
17
18

19
20 **Leaf Fraction.** The LF values were significantly higher for the infant FC networks than for the random
21 networks. The BAND×NETWORK TYPE interaction was significant, because unlike for random networks, LF
22 significantly varied across frequency bands for the infant FC networks ($p < .001$ in all pairwise comparisons
23 between the gamma and any other band as well as between the delta/beta and the theta/lower-alpha/higher-
24 alpha comparisons).
25
26

27
28 **Diameter.** The DIAM values were significantly lower for the infant FC networks than for the random
29 networks. The BAND×NETWORK TYPE interaction was significant, because unlike for random networks, DIAM
30 significantly varied across frequency bands for the infant FC networks ($p < .001$ in all pairwise comparisons
31 between the gamma and any other band as well as between the delta/beta and the theta/lower-alpha/higher-
32 alpha comparisons, except for the comparison between the delta and the beta band, which yielded a p value of
33 .1).
34
35

36
37 **Tree Hierarchy.** The TH values were significantly higher for the infant FC networks than for the random
38 networks. The BAND×NETWORK TYPE interaction was significant, because unlike for random networks, LF
39 significantly varied across frequency bands for the infant FC networks ($p < .001$ in all pairwise comparisons
40 between the gamma and any other band as well as between the delta and any other band).
41
42

43
44 Overall, all network characteristics significantly differed from those of the corresponding random
45 networks. Further, in contrast to the random networks, the characteristics of infant FC networks differed across
46 the different frequency bands. These results suggest that the infant FC networks, relative to random control
47 networks, have more integrated/star like structure.
48
49
50
51
52
53
54
55
56
57
58
59
60

3.2. Scalp distribution of Betweenness Centrality and Degree Centrality

Figure 3 (left panel) shows the scalp distribution of the BC values, separately for the different frequency bands. The main effect of NODE LOCATION was significant for all frequency bands (see detailed results in Table 3). Post-hoc comparisons indicated a parietal maximum in the delta, midline fronto-central maximum in the theta, midline frontal maximum in the lower alpha, centro-temporal maximum in the higher alpha, and lateral fronto-temporal maxima in the beta and gamma bands ($p < .001$ in most comparisons). Figure 3 (right panel) shows the scalp distribution of the DEG values, separately for the different frequency bands. The main effect of NODE LOCATION was significant in all frequency bands (see detailed results in Table 3). Post-hoc comparisons indicated temporo-parietal maximum in the delta, midline fronto-central maximum in the theta, midline fronto-central and temporo-parietal maxima in the lower and upper alpha, and lateral fronto-temporal maxima in the beta and gamma bands ($p < .001$ in most comparisons, see Table 3).

PLEASE INSERT FIGURE 3 HERE

3.3. Relationship between network characteristics and medical/biological measures

Table 4 and Figure 4 summarize the significant results yielded by the linear regression models. For the delta band we have found only one significant regression model, with GA explaining $R^2 = 3\%$ of the variance accounted for MaxBC. For the beta, and gamma bands no significant linear regression models were obtained.

Linear regression models for the theta (4.0-8.0 Hz) frequency band. In the theta frequency band, MaxDeg had $R^2 = 6\%$, LF had $R^2 = 5\%$, and DIAM had $R^2 = 4\%$ of the variance accounted for by Gestation Age length (GA). TH had $R^2 = 8\%$ of the variance explained by GA and Mother's height (MH). Thus, MST network characteristics in the theta band were mainly associated with GA.

Linear regression models for the lower alpha (8.0-10.0 Hz) frequency band. In the lower alpha frequency band, LF had $R^2 = 5\%$ and TH had $R^2 = 4\%$ of the variance accounted for by GA. DIAM had $R^2 = 3\%$ of the variance explained by GA. Thus, similarly to theta frequency band, MST network characteristics in the lower alpha band were mainly associated with GA.

Linear regression models for the upper alpha (10.0-13.0 Hz) frequency band. In the upper alpha frequency band, MaxDeg had $R^2 = 5\%$, LF had $R^2 = 8\%$, and TH had $R^2 = 7\%$ of the variance accounted for by GA. MaxBC had $R^2 = 7\%$ while DIAM had $R^2 = 12\%$ of the variance explained by GA and Mother's age (MA). Thus again, MST network characteristics in the upper alpha band were mainly associated with GA, while MA has also appeared in two models.

1
2
3 Overall, these results suggest that GA affects the properties of neonatal infant FC networks in the theta,
4 lower and upper alpha bands (see Figure 4). Colinearity measures showed no significant collinearity when two
5 medical/biological variables appeared in the same model: tolerance, which is the percent of variance in
6 independent variables not explained by other independent variables, was always greater than $1-R^2$, suggesting
7 that our predictors were not redundant.
8
9
10

11 PLEASE INSERT FIGURE 4 HERE
12
13
14
15
16

17 Discussion

18
19 The aim of the present study was to characterize the topological organization of the human large-scale
20 EEG-based FC in a large sample of healthy full-term neonates. By comparing the brain FC network topology with
21 referential random networks, the presence of an early cost-efficient organization and hierarchical architecture has
22 been demonstrated in all EEG frequency bands. The results also suggested that the FC networks of theta and
23 alpha oscillations are characterized by a more optimal ratio between functionally segregated and integrated
24 neuronal communication than those appearing in the other frequency bands. We found that fronto-central and
25 parieto-central sites appear to be the main hubs of these networks. Furthermore, some characteristics of the
26 theta- and alpha-band FC network topologies were found to be associated with gestational age. This suggests
27 that individual differences in the functional network organization are related to the level of cortical maturity at
28 birth. Results are discussed in detail in the following sections.
29
30
31
32
33
34
35

36 Topology of functional networks in newborn infants

37
38
39 FC networks extracted from the EEG of newborn infants in quiet sleep were compared to referential
40 random networks (constructed by randomly rewiring graphs connections). In all studied EEG frequency bands
41 (delta, theta, lower and higher alpha, beta and gamma), the empirically obtained FC networks exhibited
42 significantly higher maximal degree (MAXDEG) and betweenness centrality (MAXBC), tree hierarchy (TH), and
43 leaf fraction (LF) together with lower diameter (DIAM) relative to random networks. These results suggest that the
44 organization of the neuronal communication follows a hierarchical pattern (high TH) composed of some densely
45 connected nodes (high MAXBC and MAXDEG) with the majority of nodes serving as periphery within the network
46 (high LF). Low path length promote long range connections optimized for maximal processing speed, while high
47 clustering support high level of local connectivity optimized for minimal wiring cost and resilience [Watts and
48 Strogatz, 1998]. MST diameter positively correlates with the path length and with the clustering coefficients while
49 the leaf fraction is negatively associated with path length and positively with clustering [Tewarie et al., 2015].
50 Random networks have low clustering and a short average path length while networks in a regular, lattice-like
51
52
53
54
55
56
57
58
59
60

1
2
3 configuration are characterized by high clustering and a long average path length [Stam et al., 2014; Bullmore
4 and Sporns, 2009]. Finally, scale free networks with star like topology combine the lower path length compared to
5 regular or random networks but lower clustering than regular. Scale-free networks are characterized by the
6 relative commonness of nodes with a degree that greatly exceeds the average [so-called hub nodes; Barabasi
7 and Albert, 1999]. Our findings suggest that the neonatal FC networks show scale free network organizational
8 principles, which are thus likely to be present from an early stage of the cortical connectome. In line with our
9 findings, a similar study in 5- 7 years old children showed that their FC networks display a star-like centralized
10 topology which shifts toward more ordered configuration by development [Boersma et al., 2013]. The current
11 results of the early architecture of the functional connectome is consistent with studies reporting small-world
12 modular topological properties in infants, children, and adults [Otte et al., 2015; Omidvarnia et al. 2014; Boersma
13 et al., 2011; Boersma et al., 2013; Fair et al., 2008; Power et al., 2010; Supekar et al., 2009; Bassett and
14 Bullmore, 2006; Bathelt et al., 2013; Hagmann et al., 2010; Bullmore and Sporns, 2009; Tymofiyeva et al., 2013].

15
16 We also found that the topology of the FC networks obtained for the theta and alpha frequency bands
17 characteristically differed from those of the other frequency bands suggesting the emergence of distinct FCs
18 already at birth. The networks in theta and alpha rhythms displayed lower level of MAXBC, TH, and LF with
19 higher DIAM relative to the gamma-, beta-, and delta-band networks. These results indicate that theta- and
20 alpha-band FC networks are shifted towards the regular network topology with more ordered chain-like
21 configuration and higher level clustering. This topology favors the segregation of subnetworks. Therefore these
22 functional networks are better suited for local processes versus the networks working in the other bands.
23 Concordant to our results, Omidvarnia and collages [2014] obtained evidence supporting a similar frequency-
24 specific network organization. Specifically, they found that for theta and alpha oscillations, the level of clustering
25 in the precentral regions and general modularity were higher in full-term relative to preterm newborns, suggesting
26 developmental changes during late gestation at these frequency bands. Oscillations in different frequency bands
27 are often linked to different physiological mechanisms: slower oscillations associated with variation in large-scale
28 excitability (probably through neuromodulation, Miller, 2009), while higher-frequency oscillations were reported to
29 correspond to local field potentials [Buzsáki and Draguhn, 2004]. It has been proposed that the emergence of
30 discrete bands in infancy and childhood may reflect the maturation of distinct cortical generators producing the
31 observed rhythms [Bollimunta et al., 2011] and the processes of synaptogenesis and pruning [Tarokh et al.,
32 2010; Tarokh et al., 2011; Kurth et al., 2010, for review see Uhlhaas et al., 2009].

33 34 35 36 37 38 39 40 41 42 43 44 45 46 47 48 49 50 51 52 53 **Topography of functional networks in newborn infancy**

54
55 The observed high nodal centrality (MAXBC and MAXDEG) of the newborn brain networks indicates that
56 most information is routed via a few central nodes. These hub nodes serve the integration of the functional
57
58
59
60

1
2
3 networks. Figure 3 shows that midline frontal, central and posterior electrodes displayed the highest BC and DEG
4 values in the lower frequency-band (delta to low alpha) MSTs. Lateral temporal electrodes were most likely to
5 serve as hubs in the MSTs for faster bands (beta and gamma bands) with the high-alpha band BC and DEG
6 showing an intermediate scalp distribution pattern. It is important to note that although spatial resolution of the
7 present EEG recording was limited, clear spatial specificity of hub nodes in low versus high frequency oscillations
8 was demonstrated. Analysis of MST graphs on a large sample of EEG data (N=227) recorded from 5-7 years old
9 children showed similar fronto-parietal dominance of BC and DEG, and the connectivity strength further
10 increased between these hub nodes during development [Boersma, 2013]. The hub regions observed here also
11 overlap with both structural and functional hub regions as reported for the adult brain [Hagmann et al., 2008; Hoff
12 et al., 2013; Bulmore and Sporns, 2009]. This suggests an early presence of connectivity hubs in the human
13 brain. Our results are compatible with evidence about the topography of FC in pre- and full-term newborns
14 (Omidvarnia et al. 2014). These authors showed that the anterior region exhibits the strongest clustering and
15 DEG in the theta and low alpha frequency bands. From an anatomical perspective, despite the methodological
16 differences, the midline frontal and posterior hubs of the delta-, theta- and alpha-band networks identified in the
17 present study are consistent with the main hubs regions described in the fMRI literature. Under rest/no-task
18 conditions, the functional brain network comprises the strongly interconnected medial prefrontal cortex, the
19 posterior cingulate, the inferior parietal lobe, and the lateral temporal cortices [Fox and Raichle, 2007; Fox et al.,
20 2005; Power et al., 2010; Bathelt et al., 2013]. It has been suggested that the alpha band resting state EEG
21 network is the one most likely to be associated with the default mode network [Chen et al., 2008; Knyazev et al.,
22 2015] and the frontal–parietal attention networks [Sadaghiani et al., 2012]. The crucial role of these hub nodes in
23 development is supported by findings showing that frontal and parietal areas might be affected in
24 neurodevelopmental disorders, such as autism [Courchesne and Pierce, 2005; Just et al., 2012] and attention
25 deficit/hyperactivity disorder [Tomasí and Volkow, 2011 for reviews see Uhlhaas et al., 2009; Uhlhaas et al.,
26 2010].

43 **Developmental changes of functional networks topology**

44
45
46 From the investigated variables of prenatal influences and general clinical risk factors, only GA was
47 found to be consistently associated with the FC network characteristics, mainly in the theta and alpha bands.
48 Linear regression analysis showed that functional networks of more mature infants (longer prenatal development,
49 as measured by GA) were less centralized (lower leaf number, MAXDEG, and MAXBC) and less hierarchical
50 (longer DIAM) than for infants with shorter prenatal development. Larger diameter and lower leaf number both
51 point to a more chainlike, elongated shape of the MSTs. In other words more mature infants are ahead in terms
52 of resting state network topology, having more decentralized network organization than infants with shorter
53 prenatal development time. Thus it appears that the human connectome is mainly star-like during the late
54
55
56
57
58
59
60

1
2
3 prenatal development. Possibly at about the time of birth, its functional specialization increases through
4 increased effectiveness of information transfer between neighboring nodes. These connectivity changes may
5 reflect intermediate cost efficient topology that optimizes communication without overloading central nodes by
6 segregation of sub-networks that subserve different functions and integration of areas involved in the same
7 function. The observed early architecture of the functional connectome is consistent with recent studies showing
8 a small-world organization of the infant functional brain networks as derived from EEG recordings [Omidvarnia et
9 al. 2014, Fair et al., 2008; Power et al., 2010; Supekar et al., 2009, Bassett and Bullmore 2006; Hagmann et al.
10 2008; Bullmore and Sporns 2009; Tymofiyeva et al. 2013]. Thus the current findings suggest that developmental
11 changes of FC occur as early as the third trimester of gestation (36-41 week).

12
13
14
15
16
17
18 The maturation of body systems of the human fetus including the brain's connectome genesis during the
19 last trimester of gestation are regarded as a critical period of prenatal ontogenesis [see Fransson et al. 2007;
20 Uhlhaas et al. 2010]. Our conclusion regarding the early development of FC network topology during this period
21 may thus reflect, to some extent, anatomical maturation processes, which could include ongoing growth in axonal
22 count of the cortical and thalamo-cortical pathways by white matter myelination and synaptic pruning [Volpe,
23 1995, Hermoye et al., 2006; Huttenlocher and Dabholkar, 1997]. Myelination is one of the core developmental
24 events in the late prenatal period by which maturation of the neuronal fibers in the neuronal feedback loops are
25 realized and the signal transmission speed increases [Cayre et al., 2009; Goldman et al., 1997, Bollimunta et al.,
26 2011]. The current most widely accepted theory suggests that neuronal feedback loops, comprising thalamic,
27 cortical and thalamo-cortical relay cells and GABAergic interneurons play an important role in the generation and
28 synchronization of brain oscillations [for review see Uhlhaas et al. 2010, Fritschy, 2008; Le Magueresse and
29 Monyer, 2013]. Thus, one may hypothesize that structural and functional connectivity between regions develops
30 similarly with the maturation of the neuronal fibers in these areas.

31
32
33
34
35
36
37
38
39
40
41
42
43
44
45
46
47
48
49
50
51
52
53
54
55
56
57
58
59
60
Previous cross-sectional studies investigating the strength of cortical coupling in relation to prenatal
development reported stronger FC in fronto-central and temporal regions in the delta and theta bands [González
et al., 2011; Dulce et al., 2007, Omidvarnia et al. 2014] in full-term compared to preterm infants. Further, weaker
coupling of the posterior areas in the delta band and lower intra-hemispheric FC in the theta and alpha bands
were observed in full-term than in preterm neonates [Batuev et al., 2008]. However the few existing longitudinal
studies measuring FC topology in full term healthy newborns showed somewhat different associations with
gestational age. For instance, alpha-band FC was found to be weakening over time between frontal and parieto-
temporal electrode locations, while increases in fronto-occipital FC strength was associated with low medical risk
and optimal neurobehavioral measures [Duffy, Als and McAnulty, 2003]. Consistently, a follow-up study of
preterm infants reported weakening functional coupling in the theta and delta bands with gestation age and
postnatal maturation while more mature infants displayed stronger coupling at higher frequencies at occipital
recording sites (Meijer et al., 2014). These discrepancies between the findings of cross-sectional and longitudinal

1
2
3 studies could be explained by the assumption of Thatcher [Thatcher et al., 2008; Thatcher, 1992], who suggested
4 that development in children is programmed in cycles with periods of increasing and decreasing coherence which
5 have different on- and offsets in different regions. The current results are compatible with this hypothesis.
6
7

8 We speculate that the gradual decentralization of the neuronal networks with maturation may be related
9 to the partial switching from thalamo-cortical to cortico-cortical dominance of neuronal network, which leads to the
10 emergence of higher FC strength in function-differentiated cortical areas (such as the primary sensory cortical
11 areas). This would appear in the EEG measures as a weakening of the strong FC connectivity of the most
12 overloaded hub regions in the midline fronto-posterior areas (indexed by decreasing BC and DEG) after prenatal
13 development, in line with the previously observed weakening of both long-range and local posterior connectivity
14 [Duffy, Als and McAnulty, 2003; Meijer et al., 2014; Batuev et al. 2008]. Pruning or elimination of some non-
15 optimal connections of the thalamo-cortical networks may underlie this developmental change. This idea also is
16 compatible with the suggestion by Thatcher who argued that development involves local excessive production of
17 synaptic connections followed by pruning of the unused connections [Thatcher et al., 2009; Thatcher, 1992].
18
19
20
21
22
23
24

25 **Limitation and future directions**

26
27
28 The present study provided data describing the general characteristics and developmental changes in global
29 network integrity of the neonatal brain. Neural network analysis may provide a functional biomarker for monitoring
30 clinical conditions in newborn infants. Further longitudinal studies are needed to establish the relationship
31 between early brain network organization and later neurocognitive development. It is important to note that most
32 studies assessing infant brain activity by electrophysiological means (including the current one) have limited
33 spatial resolution due to practical limitations (Tokariev et al., 2015). Simultaneous fMRI and electrophysiological
34 recoding could potentially improve our understanding of the joint development of structural and functional
35 connectivity the infant brain.
36
37
38
39
40
41

42 **Acknowledgements**

43
44 This work was funded by the Hungarian Academy of Sciences [MTA] post-doctoral fellowship to B.T. and the
45 Hungarian National Research Fund [OTKA] projects K101060 and K115385 to I.W. The authors declare no
46 actual or potential conflict of interest. All authors have reviewed the contents of the submitted manuscript,
47 approve of its contents and the accuracy of the data.
48
49
50
51
52
53
54
55
56
57
58
59
60

References

- 1
2
3
4
5 Achard S, Salvador R, Whitcher B, Suckling J, Bullmore ED (2006): A resilient, low-frequency, small-world
6 human brain functional network with highly connected association cortical hubs. *J Neurosci* 26(1): 63-72.
7
8 *doi:10.1523/JNEUROSCI.3874-05.2006*
9
10
11 Anders TF, Emde RN, Parmelee AH (1971): A manual of standardized terminology, techniques and criteria for
12 scoring of states of sleep and wakefulness in newborn infants. UCLA Brain Information Service/BRI
13 Publications Office, NINDS Neurological Information Network.
14
15
16
17 Barabási AL, Albert R (1999): Emergence of scaling in random networks. *Science* 286(5439): 509-512.
18
19 *doi:10.1126/science.286.5439.509*
20
21
22 Bassett DS, Bullmore ED (2006): Small-world brain networks. *Neuroscientist*, 12(6): 512-523.
23
24 *doi:10.1177/1073858406293182*
25
26
27 Bassett DS, Bullmore ET, Meyer-Lindenberg A, Apud JA, Weinberger DR, Coppola R (2009): Cognitive *fitness* of
28 cost-efficient brain functional networks. *Proc Natl Acad Sci U S A* 106(28): 11747-11752.
29
30 *doi:10.1073/pnas.0903641106*
31
32
33 Bathelt J, O'Reilly H, Clayden J D, Cross J H, de Haan M (2013): Functional brain network organisation of
34 children between 2 and 5 years derived from reconstructed activity of cortical sources of high-density
35 EEG recordings. *Neuroimage* 82: 595-604. *doi:10.1016/j.neuroimage.2013.06.003*
36
37
38
39 Batuev AS, Iovleva NN, Koshchavtsev AG (2008): Comparative analysis of the EEG in babies in the first month
40 of life with gestation periods of 30–42 weeks. *Neurosci Behav Physiol* 38(6): 621-626.
41
42 *doi:10.1007/s11055-008-9018-1*
43
44
45 Barry RJ, Clarke AR, McCarthy R, Selikowitz M, Johnstone SJ, Rushby JA (2004): Age and gender effects in
46 EEG coherence: I. Developmental trends in normal children. *Clin Neurophysiol* 115(10): 2252-2258.
47
48 *doi:10.1016/j.clinph.2004.05.004*
49
50
51 Boersma M, Smit DJ, Boomsma DI, De Geus EJ, Delemarre-van de Waal HA, Stam CJ (2013): Growing trees in
52 child brains: graph theoretical analysis of electroencephalography-derived minimum spanning tree in 5-
53 and 7-year-old children reflects brain maturation. *Brain Connect* 3(1): 50-60.
54
55 *doi:10.1089/brain.2012.0106*
56
57
58
59
60

- 1
2
3 Boersma M, Smit DJ, de Bie H, Van Baal GCM, Boomsma DI, de Geus EJ, Delemarre-van de Waal HA, Stam,
4 CJ (2011): Network analysis of resting state EEG in the developing young brain: structure comes with
5 maturation. *Hum Brain Mapp* 32(3): 413-425. doi:10.1002/hbm.21030
6
7
8
9 Bollimunta A, Mo J, Schroeder CE, Ding M (2011): Neuronal mechanisms and attentional modulation of
10 corticothalamic alpha oscillations. *J Neurosci* 31(13): 4935-4943. doi:10.1523/JNEUROSCI.5580-
11 10.2011
12
13
14
15 Bullmore E, Sporns O (2009): Complex brain networks: graph theoretical analysis of structural and functional
16 systems. *Nat Rev Neurosci* 10(3): 186-198. doi:10.1038/nrn2575
17
18
19 Buzsáki G, Draguhn A (2004): Neuronal oscillations in cortical networks. *Science* 304(5679): 1926-1929.
20 doi:10.1126/science.1099745
21
22
23
24 Cayre M, Canoll P, Goldman JE (2009): Cell migration in the normal and pathological postnatal mammalian
25 brain. *Prog Neurobiol* 88(1): 41-63. doi:10.1016/j.pneurobio.2009.02.001
26
27
28
29 Chen AC, Feng W, Zhao H, Yin Y, Wang P (2008): EEG default mode network in the human brain: spectral
30 regional field powers. *Neuroimage* 41(2): 561-574. doi:10.1016/j.neuroimage.2007.12.064
31
32
33 Courchesne E, Pierce K (2005): Brain overgrowth in autism during a critical time in development: implications for
34 frontal pyramidal neuron and interneuron development and connectivity. *Int J Dev Neurosci* 23(2): 153-
35 170. doi:10.1016/j.ijdevneu.2005.01.003
36
37
38
39 de Haan W, van der Flier WM, Koene T, Smits LL, Scheltens P, Stam CJ (2012): Disrupted modular brain
40 dynamics reflect cognitive dysfunction in Alzheimer's disease. *Neuroimage* 59(4): 3085-3093.
41 doi:10.1016/j.neuroimage.2011.11.055
42
43
44
45 Dulce M, Mañas S, Pereda E, Garrido J, López S, De Vera L, González JJ (2007): Maturation changes in the
46 interdependencies between cortical brain areas of neonates during sleep. *Cereb Cortex* 17(3): 583-590.
47 doi:10.1093/cercor/bhk002
48
49
50
51 Duffy FH, Als H, McAnulty GB (2003): Infant EEG spectral coherence data during quiet sleep: unrestricted
52 principal components analysis—relation of factors to gestational age, medical risk, and neurobehavioral
53 status. *Clin EEG Neurosci* 34(2): 54-69. doi:10.1177/155005940303400204
54
55
56
57
58
59
60

- 1
2
3 Fair DA, Cohen AL, Dosenbach NU, Church JA, Miezin FM, Barch DM, Raichle ME, Petersen SE, Schlaggar BL
4 (2008): The maturing architecture of the brain's default network. *Proc Natl Acad Sci U S A* 105(10):
5 4028-4032. doi:10.1073/pnas.0800376105
6
7
8
9 Ferreira LK, Busatto GF (2013): Resting-state functional connectivity in normal brain aging. *Neurosci Biobehav*
10 *Rev* 37(3): 384-400. doi:10.1016/j.neubiorev.2013.01.017
11
12
13 Fritschy JM (2008): Epilepsy, E/I balance and GABAA receptor plasticity. *Front Mol Neurosci* 1(5): 1-6.
14 doi:10.3389/neuro.02.005.2008
15
16
17
18 Fransson P, Skiöld B, Horsch S, Nordell A, Blennow M, Lagercrantz H, Åden U (2007): Resting-state networks in
19 the infant brain. *Proc Natl Acad Sci U S A* 104(39): 15531-15536. doi:10.1073/pnas.0704380104
20
21
22
23 Fox MD, Raichle ME (2007): Spontaneous fluctuations in brain activity observed with functional magnetic
24 resonance imaging. *Nat Rev Neurosci* 8(9): 700-711. doi:10.1038/nrn2201
25
26
27 Fox MD, Snyder AZ, Vincent JL, Corbetta M, Van Essen DC, Raichle ME (2005): The human brain is intrinsically
28 organized into dynamic, anticorrelated functional networks. *Proc Natl Acad Sci U S A* 102(27): 9673-
29 9678. doi:10.1073/pnas.0504136102
30
31
32
33 Gelman A, Hill J, Yajima M (2012): Why we (usually) don't have to worry about multiple comparisons. *JREE* 5(2):
34 189-211. doi:10.1080/19345747.2011.618213
35
36
37
38 Goldman JE, Zerlin M, Newman S, Zhang L, Gensert J (1997): Fate determination and migration of progenitors in
39 the postnatal mammalian CNS. *Dev Neurosci* 19(1): 42-48. doi:10.1159/000111184
40
41
42
43 González JJ, Mañas S, De Vera L, Méndez LD, López S, Garrido JM, Pereda E (2011): Assessment of
44 electroencephalographic functional connectivity in term and preterm neonates. *Clin Neurophysiol* 122(4):
45 696-702. doi:10.1016/j.clinph.2010.08.025
46
47
48
49 Gong G, He Y, Concha L, Lebel C, Gross DW, Evans AC, Beaulieu C (2009): Mapping anatomical connectivity
50 patterns of human cerebral cortex using in vivo diffusion tensor imaging tractography. *Cereb Cortex*
51 19(3): 524-536. doi:10.1093/cercor/bhn102
52
53
54
55 Hagmann P, Cammoun L, Gigandet X, Meuli R, Honey CJ, Wedeen VJ, Sporns O (2008): Mapping the structural
56 core of human cerebral cortex. *PLoS Biol* 6(7): e159. doi:10.1371/journal.pbio.0060159
57
58
59
60

- 1
2
3 Hagmann P, Sporns O, Madan N, Cammoun L, Pienaar R, Wedeen VJ, Meuli R, Thiran JP, Grant PE (2010):
4 White matter maturation reshapes structural connectivity in the late developing human brain. *Proc Natl*
5 *Acad Sci U S A* 107(44): 19067-19072. doi:10.1073/pnas.1009073107
6
7
8
9 Hermoye L, Saint-Martin C, Cosnard G, Lee SK, Kim J, Nassogne MC, Menten R, Clapuyt P, Donohue PK, Hua
10 K, Wakana S, Jiang H, van Zijl PC, Mori S (2006): Pediatric diffusion tensor imaging: normal database
11 and observation of the white matter maturation in early childhood. *Neuroimage* 29(2): 493-504.
12 doi:10.1016/j.neuroimage.2005.08.017
13
14
15
16
17 Hoff GAJ, Van den Heuvel MP, Benders MJ, Kersbergen KJ, De Vries LS (2013): On development of functional
18 brain connectivity in the young brain. *Front Hum Neurosci* 7(650): 1-7. doi:10.3389/fnhum.2013.00650
19
20
21
22 Huttenlocher PR (1979): Synaptic Density in Human Frontal Cortex-Developmental Changes and Effects of
23 Aging. *Brain Res* 163: 195-205. doi:10.1016/0006-8993(79)90349-4
24
25
26 Jennekens, W., Niemarkt, H. J., Engels, M., Pasman, J. W., van Pul, C., & Andriessen, P. (2012). Topography of
27 maturational changes in EEG burst spectral power of the preterm infant with a normal follow-up at
28 2years of age. *Clin Neurophysiol* 123(11), 2130-2138.
29
30
31
32 Just MA, Keller TA, Malave VL, Kana RK, Varma S (2012): Autism as a neural systems disorder: a theory of
33 frontal-posterior underconnectivity. *Neurosci Biobehav Rev* 36(4): 1292-1313.
34 doi:10.1016/j.neubiorev.2012.02.007
35
36
37
38 Khazipov R, Luhmann HJ (2006): Early patterns of electrical activity in the developing cerebral cortex of humans
39 and rodents. *TINS* 29(7): 414-418. doi:10.1016/j.tins.2006.05.007
40
41
42
43 Knyazev GG, Volf NV, Belousova LV (2015): Age-related differences in electroencephalogram connectivity and
44 network topology. *Neurobiol Aging* 36(5): 1849-1859. doi:10.1016/j.neurobiolaging.2015.02.007
45
46
47
48 Kruskal JB (1956): On the shortest spanning subtree of a graph and the traveling salesman problem. *Proc Am*
49 *Math Soc* 7(1): 48-50. doi:10.2307/2033241
50
51
52 Kurth S, Ringli M, Geiger A, LeBourgeois M, Jenni OG, Huber R (2010): Mapping of cortical activity in the first
53 two decades of life: a high-density sleep electroencephalogram study. *J Neurosci* 30(40): 13211-13219.
54 doi:10.1523/JNEUROSCI.2532-10.2010
55
56
57
58
59
60

- 1
2
3 Lebel C, Walker L, Leemans A, Phillips L, Beaulieu C (2008): Microstructural maturation of the human brain from
4 childhood to adulthood. *Neuroimage* 40(3): 1044-1055. doi:10.1016/j.neuroimage.2007.12.053
5
6
7 Le Magueresse C, Monyer H (2013): GABAergic interneurons shape the functional maturation of the cortex.
8 *Neuron* 77(3): 388-405. doi:10.1016/j.neuron.2013.01.011
9
10
11 Martin A, Chao LL (2001): Semantic memory and the brain: structure and processes. *Curr Opin Neurobiol* 11(2):
12 194-201. doi:10.1016/S0959-4388(00)00196-3
13
14
15
16 Meijer EJ, Hermans KHM, Zwanenburg A, Jennekens W, Niemarkt HJ, Cluitmans PJM, van Pul C, Wijn PFF,
17 Andriessen P (2014): Functional connectivity in preterm infants derived from EEG coherence analysis.
18 *Eur J Paediatr Neurol* 18(6): 780-789. doi:10.1016/j.ejpn.2014.08.003
19
20
21
22 Newman MEJ, Girvan M (2004): Finding and evaluating community structure in networks. *Phys Rev E Stat*
23 *Nonlin Soft Matter Phys* 69(2 Pt 2): 026113. doi:10.1103/PhysRevE.69.026113
24
25
26
27 Micheloyannis S, Pachou E, Stam CJ, Vourkas M, Erimaki S, Tsirka V (2006): Using graph theoretical analysis of
28 multi channel EEG to evaluate the neural efficiency hypothesis. *Neurosci Lett* 402(3): 273-277.
29 doi:10.1016/j.neulet.2006.04.006
30
31
32
33 Miller KJ, Sorensen LB, Ojemann JG, den Nijs M (2009): Power-Law Scaling in the Brain Surface Electric
34 Potential. *PLoS Comput Biol* 5(12): e1000609. doi:10.1371/journal.pcbi.1000609
35
36
37 Myers, M. M., Grieve, P. G., Izraelit, A., Fifer, W. P., Isler, J. R., Darnall, R. A., & Stark, R. I. (2012).
38 Developmental profiles of infant EEG: overlap with transient cortical circuits. *Clin Neurophysiol* 123(8),
39 1502-1511.
40
41
42
43 Pearson K (1895): Contributions to the mathematical theory of evolution. II. Skew variation in homogeneous
44 material. *Philosophical Transactions of the Royal Society of London*. A. p. 343-414.
45
46
47
48 Pereda, E., de La Cruz, D. M., Manas, S., Garrido, J. M., López, S., & González, J. J. (2006). Topography of
49 EEG complexity in human neonates: effect of the postmenstrual age and the sleep state. *Neurosci Lett*
50 394(2), 152-157.
51
52
53
54 Power JD, Fair DA, Schlaggar BL, Petersen SE (2010): The development of human functional brain networks.
55 *Neuron* 7(5): 735-748. doi:10.1016/j.neuron.2010.08.017
56
57
58
59
60

- 1
2
3 Prechtl HF (1974): The behavioural states of the newborn infant (a review): *Brain Res* 76(2): 185-212.
4 *doi:10.1016/0006-8993(74)90454-5*
5
6
7 Sadaghiani S, Scheeringa R, Lehongre K, Morillon B, Giraud AL, D'Esposito M, Kleinschmidt A (2012): Alpha-
8 band phase synchrony is related to activity in the fronto-parietal adaptive control network. *J Neurosci*
9 32(41): 14305-14310. *doi:10.1523/JNEUROSCI.1358-12.2012*
10
11
12
13 Schumacher, E. M., Stiris, T. A., & Larsson, P. G. (2015). Effective connectivity in long-term EEG monitoring in
14 preterm infants. *Clin Neurophysiol* 126(12), 2261-2268.
15
16
17
18 Smit DJ, Boersma M, Schnack HG, Micheloyannis S, Boomsma DI, Hulshoff Pol HE, Stam CJ, de Geus EJ
19 (2012): The brain matures with stronger functional connectivity and decreased randomness of its
20 network. *PLoS ONE* 7(5): e36896. *doi:10.1371/journal.pone.0036896*
21
22
23
24 Stam CJ, Nolte G, Daffertshofer A (2007): Phase lag index: assessment of functional connectivity from multi
25 channel EEG and MEG with diminished bias from common sources. *Hum Brain Mapp* 28(11): 1178-
26 1193. *doi:10.1002/hbm.20346*
27
28
29
30 Stam CJ, Tewarie P, Van Dellen E, Van Straaten ECW, Hillebrand A, Van Mieghem P (2014): The trees and the
31 forest: characterization of complex brain networks with minimum spanning trees. *Int J Psychophysiol*
32 92(3): 129-138. *doi:10.1016/j.ijpsycho.2014.04.001*
33
34
35
36 Stam CV, Van Straaten ECW (2012): The organization of physiological brain networks. *Clin Neurophysiol* 123(6):
37 1067-1087. *doi:10.1016/j.clinph.2012.01.011*
38
39
40
41 Stam CJ (2014): Modern network science of neurological disorders. *Nat Rev Neurosci* 15(10):683-95.
42
43
44 Supekar K, Musen M, Menon V (2009): Development of large-scale functional brain networks in children. *PLoS*
45 *Biol* 7(7): e1000157. *doi:10.1371/journal.pbio.1000157*
46
47
48 Omidvarnia A, Fransson P, Metsäranta M, Vanhatalo S (2014): Functional bimodality in the brain networks of
49 preterm and term human newborns. *Cereb Cortex* 24(10): 2657-2668. *doi:10.1093/cercor/bht120*
50
51
52
53 Otte WM, van Diessen E, Paul S, Ramaswamy R, Subramanyam Rallabandi VP, Stam CJ, Roy PK (2015): Aging
54 alterations in whole-brain networks during adulthood mapped with the minimum spanning tree indices:
55 the interplay of density, connectivity cost and life-time trajectory. *Neuroimage* 1(109): 171-189.
56
57
58
59
60

- 1
2
3 Tarokh L, Carskadon MA, Achermann P (2010): Developmental changes in brain connectivity assessed using the
4 sleep EEG. *Neuroscience* 171(2): 622-634. doi:10.1016/j.neuroscience.2010.08.071
5
6
7 Tarokh L, Van Reen E, LeBourgeois M, Seifer R, Carskadon MA (2011): Sleep EEG provides evidence that
8 cortical changes persist into late adolescence. *Sleep* 34(10): 1385-1393. doi:10.5665/SLEEP.1284
9
10
11 Thatcher RW (1992): Cyclic cortical reorganization during early childhood. *Brain Cogn* 20(1): 24-50.
12 doi:10.1016/0278-2626(92)90060-Y
13
14
15
16 Thatcher RW, North DM, Biver CJ (2008): Development of cortical connections as measured by EEG coherence
17 and phase delays. *Hum Brain Mapp* 29(12): 1400-1415. doi:10.1002/hbm.20474
18
19
20
21 Tewarie P, Van Dellen E, Hillebrand A, Stam CJ (2015): The minimum spanning tree: An unbiased method for
22 brain network analysis. *Neuroimage* 104: 177-188. doi:10.1016/j.neuroimage.2014.10.015
23
24
25 Tokariev, A., Videman, M., Palva, J. M., & Vanhatalo, S. (2015). Functional brain connectivity develops rapidly
26 around term age and changes between vigilance states in the human newborn. *Cer Cort* bhv219. doi:
27 10.1093/cercor/bhv219
28
29
30
31 Tomasi D, Volkow ND (2011): Functional connectivity hubs in the human brain. *Neuroimage* 57(3): 908-917.
32 doi:10.1016/j.neuroimage.2011.05.024
33
34
35
36 Tymofiyeva O, Hess CP, Ziv E, Lee PN, Glass HC, Ferriero DM, Barkovich AJ, Xu D (2013): A DTI-based
37 template-free cortical connectome study of brain maturation. *PLoS ONE* 8(5): e63310-e63310.
38 doi:10.1371/journal.pone.0063310
39
40
41
42 Uhlhaas PJ, Roux F, Rodriguez E, Rotarska-Jagiela A, Singer W (2010): Neural synchrony and the development
43 of cortical networks. *Trends Cogn. Sci. (Regul. Ed.)* 14(2): 72-80. doi:10.1016/j.tics.2009.12.002
44
45
46 Uhlhaas PJ, Roux F, Singer W, Haenschel C, Sireteanu R, Rodriguez E (2009): The development of neural
47 synchrony reflects late maturation and restructuring of functional networks in humans. *Proc Natl Acad*
48 *Sci U S A* 106(24): 9866-9871. doi:10.1073/pnas.0900390106
49
50
51
52 van den Heuvel MP, Pol HEH (2010): Exploring the brain network: a review on resting-state fMRI functional
53 connectivity. *Eur Neuropsychopharmacol* 20(8): 519-534. doi:10.1016/j.euroneuro.2010.03.008
54
55
56
57
58
59
60

1
2
3 van den Heuvel, MP, Stam CJ, Kahn RS, Pol HEH (2009): Efficiency of functional brain networks and intellectual
4 performance. *J Neurosci* 29(23): 7619-7624. doi:10.1523/JNEUROSCI.1443-09.2009
5
6

7 Varela F, Lachaux JP, Rodriguez E, Martinerie J (2001): The brainweb: phase synchronization and large-scale
8 integration. *Nat Rev Neurosci* 2(4): 229-239. doi:10.1038/35067550
9
10

11 Volpe JV (1995): *Neurology of the newborn*. (3rd ed.). Philadelphia: W. B. Saunders Company.
12
13

14 Watts DJ, Strogatz SH (1998): Collective dynamics of 'small-world' networks. *Nature* 393(6684): 440-442.
15 doi:10.1038/30918
16
17

18 Yap PT, Fan Y, Chen Y, Gilmore JH, Lin W, Shen D (2011): Development trends of white matter connectivity in
19 the first years of life. *PLoS ONE* 6(9): e24678. doi:10.1371/journal.pone.0024678
20
21
22
23
24
25
26
27
28
29
30
31
32
33
34
35
36
37
38
39
40
41
42
43
44
45
46
47
48
49
50
51
52
53
54
55
56
57
58
59
60

Figure legends

Figure 1. Schematic representation of global and node-specific network characteristics of a simple minimum spanning tree (MST). Circles indicate vertices (nodes), lines edges. Degree Centrality: quantifies the number of edges belonging to a particular node. Betweenness Centrality: fraction of all shortest paths that pass through a particular node. Leaf Fraction: quantifies the number nodes of the MST with degree one. Diameter: the length of the longest "shortest path" of the MST. Tree Hierarchy: quantifies the trade-off between large scale integration in the MST and the overload of central nodes.

Figure 2. Group-average (N = 139) MSTs of newborn infants represented as hierarchical graphs (A) and projected on the scalp (B), separately for each frequency band. The node color refers to the large-scale scalp location (red: frontal nodes; green: central nodes; blue: parietal nodes; yellow: temporal nodes). The edge colors on the head plots show the strength of functional connectivity (PLI) between nodes (see color calibration at the right side).

Figure 3. Scalp distribution of Betweenness Centrality (BC; Panel A) and Degree Centrality (DEG; Panel B), separately for each frequency band (delta: 0.5-4 Hz; theta: 4-8 Hz, lower alpha: 8-10 Hz, upper alpha: 10-12 Hz, beta: 13-30 Hz, gamma 30-45 Hz). Color calibration is shown at the right of each figure. Note that regions with high BC usually also show high DEG values.

Figure 4. Relationship between GA and network characteristics. The network characteristic is marked by the schematic diagram on the left. Diagrams represent the linear relationship between GA (x axis) and the corresponding network characteristics (y axis) shown by different colors for the different frequency bands. Dots correspond to the individual infants' data.

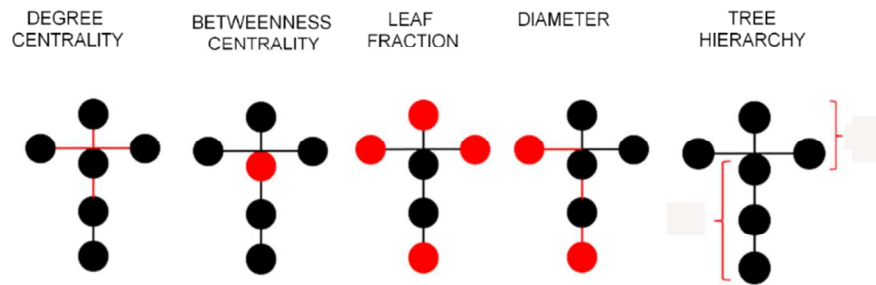


Figure 1. Schematic representation of global and node-specific network characteristics of a simple minimum spanning tree (MST). Circles indicate vertices (nodes), lines edges. Degree Centrality: quantifies the number of edges belonging to a particular node. Betweenness Centrality: fraction of all shortest paths that pass through a particular node. Leaf Fraction: quantifies the number nodes of the MST with degree one. Diameter: the length of the longest "shortest path" of the MST. Tree Hierarchy: quantifies the trade-off between large scale integration in the MST and the overload of central nodes.

86x32mm (300 x 300 DPI)

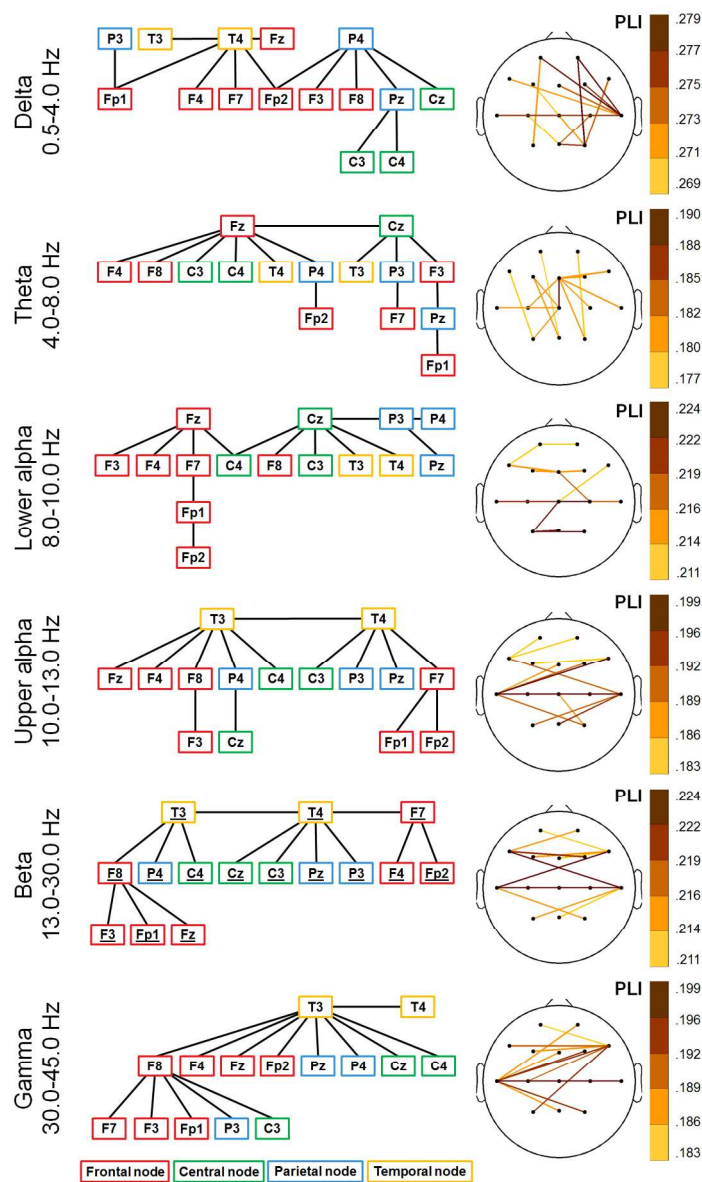
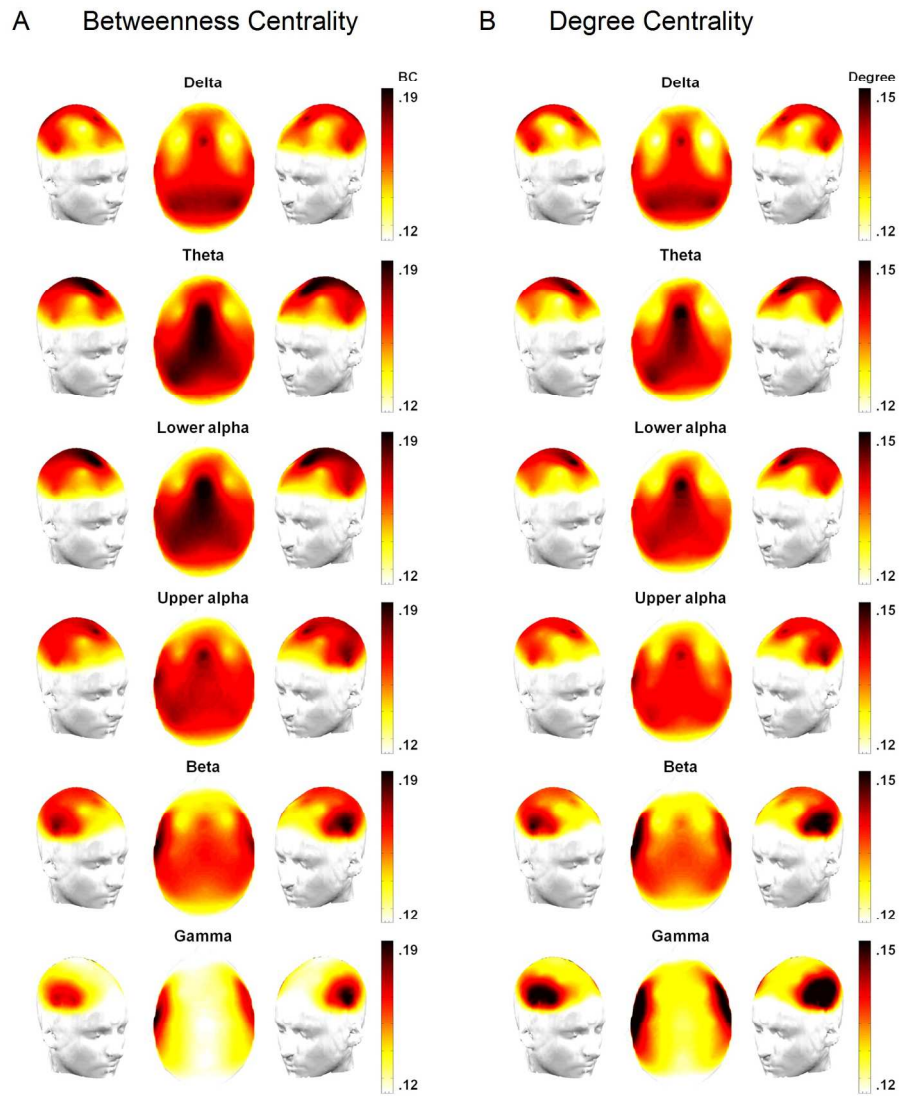


Figure 2. Group-average (N = 139) MSTs of newborn infants represented as hierarchical graphs (A) and projected on the scalp (B), separately for each frequency band. The node color refers to the large-scale scalp location (red: frontal nodes; green: central nodes; blue: parietal nodes; yellow: temporal nodes). The edge colors on the head plots show the strength of functional connectivity (PLI) between nodes (see color calibration at the right side).

140x209mm (300 x 300 DPI)



45 Figure 3. Scalp distribution of Betweenness Centrality (BC; Panel A) and Degree Centrality (DEG; Panel B),
 46 separately for each frequency band (delta: 0.5-4 Hz; theta: 4-8 Hz, lower alpha: 8-10 Hz, upper alpha: 10-
 47 12 Hz, beta: 13-30 Hz, gamma 30-45 Hz). Color calibration is shown at the right of each figure. Note that
 48 regions with high BC usually also show high DEG values.

49 562x646mm (96 x 96 DPI)

1
2
3
4
5
6
7
8
9
10
11
12
13
14
15
16
17
18
19
20
21
22
23
24
25
26
27
28
29
30
31
32
33
34
35
36
37
38
39
40
41
42
43
44
45
46
47
48
49
50
51
52
53
54
55
56
57
58
59
60

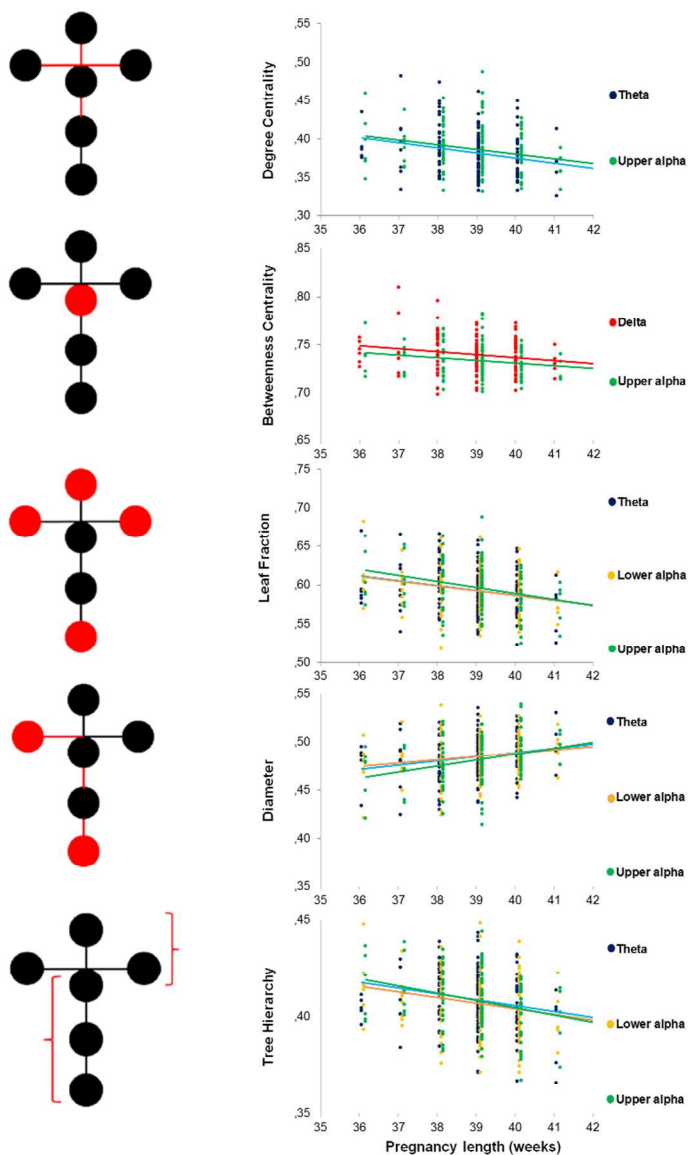


Figure 4. Relationship between GA and network characteristics. The network characteristic is marked by the schematic diagram on the left. Diagrams represent the linear relationship between GA (x axis) and the corresponding network characteristics (y axis) shown by different colors for the different frequency bands. Dots correspond to the individual infants' data.

86x114mm (300 x 300 DPI)

Table 1. Descriptive statistics of the medical/biological measures

	Missing	Mean	SD	Range	Skewness	Kurtosis
Postmenstrual age at birth (weeks)	1	38.84	1.10	36-41	-0.59	0.45
Baby's birth weight (g)	-	3321.69	396.63	2170-4160	-0.25	-0.29
Chronological age at the recording (days)	-	2.39	0.76	1-6	0.64	2.81
Mother's age (years)	1	31.45	4.47	20-43	0.27	-0.12
Mother's pre-pregnancy weight (kg)	2	66.02	12.81	42-124	1.22	2.76
Mother's postpartum weight (kg)	2	78.63	13.92	49-127	0.78	0.83
Mother's height (m)	2	1.66	0.07	1.48-1.84	0.06	0.20
Mother's systolic BP (mmHg)	3	112.63	13.30	70-160	0.42	2.40
Mother's diastolic BP (mmHg)	3	69.63	8.84	50-100	1.19	2.72

Note. The mother's pre-pregnancy weight and the length of the pregnancy were based on self-reports. *BP* = blood pressure.

Table 2. MST network characteristics and their comparison between actual and random functional networks, separately for the different frequency bands.

Descriptives				ANOVA Results					
Variable	Band	Mean	SD	Effect	ϵ	F	df	p	η^2
MaxDEG	Delta	.4028	.0345	NETWORK TYPE		3209.56	1,138	***	.96
	Theta	.3825	.0311	BAND	.29	117.01	5,690	***	.46
	Lower alpha	.3845	.0283	Interaction	.29	127.77	5,690	***	.48
	Upper alpha	.3869	.0298						
	Beta	.3997	.0383						
	Gamma	.4527	.0473						
MaxBC	Delta	.6874	.0175	NETWORK TYPE		3605.91	1,138	***	.96
	Theta	.6773	.0157	BAND	.73	123.13	5,690	***	.47
	Lower alpha	.6792	.0144	Interaction	.71	128.60	5,690	***	.48
	Upper alpha	.6814	.0149						
	Beta	.6904	.0193						
	Gamma	.7204	.0229						
LF	Delta	.6124	.0316	NETWORK TYPE		4751.59	1,138	***	.97
	Theta	.5941	.0306	BAND	.40	126.10	5,690	***	.48
	Lower alpha	.5933	.0294	Interaction	.43	144.39	5,690	***	.51
	Upper alpha	.5970	.0298						
	Beta	.6086	.0354						
	Gamma	.6622	.0434						
Diam	Delta	.4693	.0240	NETWORK TYPE		5502.26	1,138	***	.98
	Theta	.4838	.0230	BAND	.65	130.50	5,690	***	.49

	Lower alpha	.4844	.0219	Interaction	.68	156.03	5,690	***	.53
	Upper alpha	.4808	.0235						
	Beta	.4679	.0275						
	Gamma	.4217	.0326						
TH	Delta	.4472	.0164	NETWORK TYPE		4946.51	1,138	***	.97
	Theta	.4404	.0171	BAND	.72	40.99	5,690	***	.23
	Lower alpha	.4384	.0171	Interaction	.79	44.26	5,690	***	.24
	Upper alpha	.4397	.0160						
	Beta	.4422	.0170						
	Gamma	.4611	.0192						

Note. The presence of ϵ indicates the employment of Greenhouse-Geisser correction due to sphericity violation.

*** $p < .001$

1
2
3
4
5
6
7
8
9
10
11
12
13
14
15
16
17
18
19
20
21
22
23
24
25
26
27
28
29
30
31
32
33
34
35
36
37
38
39
40
41
42
43
44
45
46
47
48
49
50
51
52
53
54
55
56
57
58
59
60

For Peer Review

Table 3. The effects (ANOVA results) of Node Location on the Betweenness Centrality and Degree Centrality MST network characteristics, separately for the different frequency bands.

	BAND	F	df	p	η^2
Max BC	Delta	21.225	14, 19	***	.133
	Theta	21.663	14, 19	***	.136
	Lower alpha	23.043	14, 19	***	.143
	Upper alpha	15.741	14, 19	***	.111
	Beta	17.250	14, 19	***	.178
	Gamma	29.957	14, 19	***	.188
Max Deg	Delta	21.337	14, 19	***	.134
	Theta	21.462	14, 19	***	.135
	Lower alpha	21.073	14, 19	***	.132
	Upper alpha	14.518	14, 19	***	.095
	Beta	18.997	14, 19	***	.121
	Gamma	32.007	14, 19	***	.188

Table 4. Summary of the linear regression model results.

	MaxDEG	MaxBC	LF	DIAM	TH
Delta band					
β of Pregnancy length		-.18*			
t, df of Pregnancy length		-2.10 (134)			
R ²		.03			
df, error, df of model		1,133			
F		7.73*			
Theta band					
β of Pregnancy length	-.24**		-.22*	.21*	-.23*
t, df of Pregnancy length	-2.78 (132)		-2.46 (132)	2.46 (132)	-2.68 (131)
β of Mother's height					.19*
t, df of Mother's height					2.30 (131)
R ²	.06		.05	.04	.08
df, error, df of model	1,132		1,132	1,132	1,131
F	7.73**		6.74*	6.07*	5.75**
Lower alpha band					
β of Pregnancy length			-.22*	.18*	-.19*
t, df of Pregnancy length			-2.63 (132)	2.10 (134)	-2.26 (132)
R ²			.05	.03	.04
df, error, df of model			1,132	1,133	1,132
F			6.90*	4.39*	5.10*
Upper alpha band					
β of Pregnancy length	-.23**	-.22*	-.28***	.33***	-.27**
t, df of Pregnancy length	-2.69 (132)	-2.59 (131)	-3.38 (132)	3.94 (131)	-3.23 (132)
β of Mother's age		-.19*		.02*	
t, df of Mother's age		-2.21 (131)		2.35 (131)	

1
2
3
4
5
6
7
8
9
10
11
12
13
14
15
16
17
18
19
20
21
22
23
24
25
26
27
28
29
30
31
32
33
34
35
36
37
38
39
40
41
42
43
44
45
46
47
48
49
50
51
52
53
54
55
56
57
58
59
60

R ²	.05	.07	.08	.12	.07
df, error df of model	1,132	1,131	1,132	1,132	1,132
F	10.42**	5.01**	11.45***	9.31***	10.42**

Note. * p < .05 ** p < .01 *** p < .001. In the F row, the asterisks indicate the level of significance for the final regression model. In the β rows of the biomedical variables, the asterisks indicate the level of significance of the independent predictive power of the variable, separately.

For Peer Review